

Secondary-electron yield in the interaction of ultrarelativistic electrons and positrons with single crystals

V. I. Vit'ko and G. D. Kovalenko

Khar'kov Physicotechnical Institute, Academy of Sciences of the Ukrainian SSR

(Submitted 21 March 1988)

Zh. Eksp. Teor. Fiz. **94**, 321–327 (October 1988)

The yield of low-energy ($E < 0.1$ keV) and high-energy ($E > 0.1$ keV) electrons from silicon single crystals with thicknesses $t = 8, 30, 80, 180, 250, 460,$ and $920 \mu\text{m}$ as 1.2-GeV electrons and positrons pass through the crystals has been studied. The electron yield from the crystals has been found as a function of the crystal thickness and the orientation of the [111] axis with respect to the direction of the electron or positron beam. The experimental results are compared with calculations. Electron and positron dechanneling lengths are determined for the [111] axis and the (110) plane.

INTRODUCTION

As ultrarelativistic electrons and positrons interact with matter, inelastic collisions with atoms of the matter and scattering by atomic electrons, among other processes, occur. These two processes have been studied in detail by Bethe and Molière (see Ref. 1, for example). The collisions change the energy and momentum of the primary particles. At the same time, some of the electrons of the matter acquire an energy sufficient to escape from it (electrons are emitted from the matter). This phenomenon is widely used in order to detect currents of charged particles.^{2,3}

The emission of electrons from a single crystal and from an amorphous material differ substantially. In a single crystal, for example, the emission of the electrons is found to depend on the orientation of the crystal and the sign of the charge of the primary particles.^{4–6} By studying the yield of secondary electrons as a function of the thickness and orientation of a single crystal one can learn about kinetic processes associated with the motion of the primary particles in the crystal.

In this paper we are reporting a study of the secondary-emission yield for various thicknesses and orientations of silicon single crystals as ultrarelativistic electrons and positrons pass through them.

EXPERIMENTAL PROCEDURE

The experiments were carried out in a linear electron accelerator. The layout is shown in Fig. 1. A beam of electrons (or positrons) with an energy of 1.2 GeV is directed onto a silicon single crystal (the emitter), which is flanked on two sides by ring-shaped collectors with an inside diameter of 14 mm. The distance between the emitter and the collector is 5 mm. Those electrons which are produced as the result of elastic and inelastic interactions escape from the target, and the target acquires a positive potential with respect to ground. The amount of charge which is carried off is found from the current required to cancel the potential on the crystal. The current of the main beam is measured with a Faraday cup. The collectors are used to produce a blocking or extracting potential.

This system of an emitter and collectors is mounted in a goniometer, which can rotate the system around vertical and horizontal axes and orient it within an error of $5 \cdot 10^{-5}$ rad. Three such systems can be placed in the goniometer simulta-

neously. The systems are brought into the beam by rotating them through 120° around the beam axis.

In experiments we used silicon single crystals with thicknesses of 8, 30, 80, 180, 250, 460, and $920 \mu\text{m}$, cut in such a way that the [111] axis ran perpendicular to the geometric plane of the crystal. As was shown in Refs. 4 and 6, the electron emission current depends strongly on the voltage applied to the collectors. A curve of the emission current versus the voltage exhibits two clearly defined plateaus, at $U > 40$ V (an extracting potential) and $U < -40$ V (a blocking potential). In the case of the extracting potential we detect the total yield of emission electrons; in the case of a blocking potential we detect the yield of high-energy electrons alone. The difference between these yields is the yield of low-energy electrons, with $E \leq 100$ eV. Since the collectors in the system are separate, we can find the contribution of low-energy electrons from the first and second surfaces of the crystal with respect to the beam incidence direction.

YIELD OF LOW-ENERGY AND HIGH-ENERGY ELECTRONS

Figure 2 shows the results of these measurements of the yield of low-energy electrons from crystals of various thicknesses, for both electrons and positrons, normalized to the initial electron (or positron) current. The straight lines in this figure are least-squares fits of the experimental points. Line 1 shows the yield of low-energy electrons from the first and second surfaces; line 2 shows that from the first surface alone; and line 3 shows that from the second surface alone. The low-energy electrons from the first surface constitute 64% of the total emission, while those from the second surface constitute 36%, in good agreement with results found previously⁷ for an amorphous aluminum target. The difference in the yields from the first and second surfaces results from a density effect, because of which the field of the incoming particle is screened by atoms of the target. The field of the

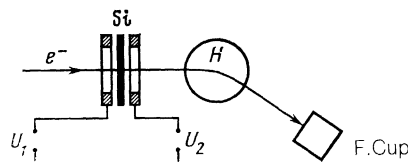


FIG. 1. Experimental layout.

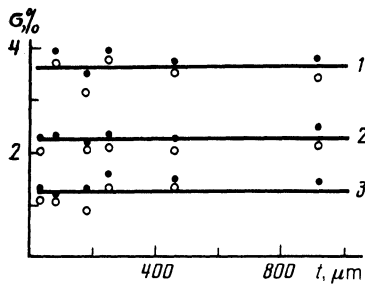


FIG. 2. Yield of low-energy electrons ($E < 100$ eV) versus the thickness of the silicon crystal during the passage of (●) electrons and (○) positrons with an energy of 1.2 GeV, normalized to a single incident particle. 1—Yield from the first and second surfaces; 2—yield from the first surface; 3—yield from the second surface.

incoming particle in vacuum as it crosses the first surface and enters the crystal is stronger than the corresponding field as the particle crosses the second surface of the crystal and emerges from it. Accordingly, the low-energy emission from the first surface of the crystal (backward emission) is more intense than that from the second surface (forward emission in terms of the direction of the beam). The fact that the low-energy yield becomes constant at $8 \mu\text{m}$ indicates that the screening of the field of the ultrarelativistic particles occurs over distances less than $8 \mu\text{m}$. The yield of low-energy electrons does not depend on the sign of the charge of the primary particle, the target thickness, or the orientation of the crystal, confirming the conclusion reached in Ref. 4: that low-energy electrons are produced primarily as a result of remote collisions and are emitted from a layer of thickness $\sim 100 \text{ \AA}$.

Figure 3 shows the yield of high-energy electrons versus the crystal thickness for an initial energy of 1.2 GeV for electrons and positrons for a disoriented crystal and for a crystal oriented with its [111] axis along the beam axis. The solid curve here approximates the experimental points for the disoriented crystal by the function $\sigma = 0.23t^{0.43}$ [%], where t is the crystal thickness in microns. The dashed curve shows the results of a Monte Carlo calculation which incorporates absorption of electrons in the target. The calculations ignored the crystal structure of the target. An analytic

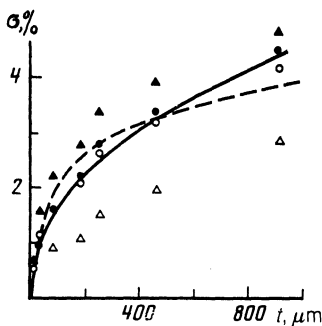


FIG. 3. Yield of high-energy electrons, normalized to a single incident particle, versus the thickness of the silicon crystal. ○—Positrons, for a disoriented crystal; ●—electrons, for a disoriented crystal; ▲—electrons, for a crystal oriented with its [111] axis along the beam axis; △—positrons, for a crystal in the same orientation. Solid curve) Approximation of the experimental points for a disoriented crystal by the function $\sigma = 0.23t^{0.43}$ [%]; dashed curve) Monte Carlo calculation incorporating absorption for a disoriented crystal.

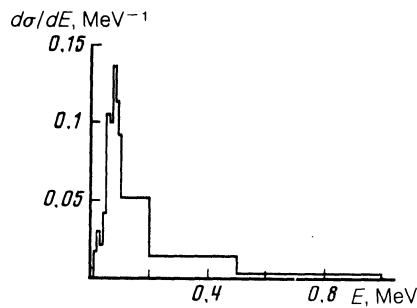


FIG. 4. Theoretical spectrum of the high-energy electrons emitted from a disoriented silicon crystal of thickness $t = 80 \mu\text{m}$.

theory predicts a functional dependence $\sigma \propto t^{0.5}$ for the yield of high-energy electrons as a function of the target thickness.⁸ It can thus be assumed that the experimental data for the disoriented crystal agree well with the values calculated from the analytic theory and by the Monte Carlo method. Figure 4 shows a Monte Carlo calculation of the spectrum of high-energy electrons emitted from a disoriented crystal with a thickness $t = 80 \mu\text{m}$. This spectrum has a maximum at 50–100 keV. The low yield of electrons with lower energies is a consequence of the absorption of these electrons in the target.

For crystals oriented with their [111] axis along the beam axis, the yield of high-energy electrons depends on the sign of the charge of the initial particles. For the electrons, the yield is higher than that from the disoriented crystal; for the positrons, it is instead lower. The reason for this sensitivity to the sign of the charge in the case of the oriented crystal lies in the nature of the motion of the initial particles. Channeled positrons move far from nuclei, so they are in a region of low electron density, and the yield of electrons is correspondingly reduced. Channeled electrons move near the nuclei, in a region of a high electron density; the number of collisions is higher, as is the yield of electrons from the crystal.

DECHANNELING LENGTHS OF ELECTRONS AND POSITRONS

Figures 5 and 6 show the difference Δ between the yields of high-energy electrons from oriented and disoriented crystals for the [111] axis and the (110) plane as a func-

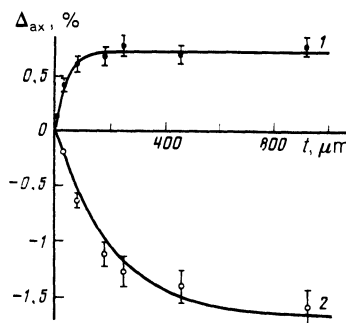


FIG. 5. Difference between the yields of high-energy electrons from a crystal oriented with its [111] axis along the beam axis and from a disoriented crystal versus the thickness of the crystals, normalized to a single incident particle. ●—Electrons; ○—positrons. Lines 1 and 2 are approximations of the experimental points by the function $\Delta = \Delta_0[1 - \exp(-t/\lambda)]$.

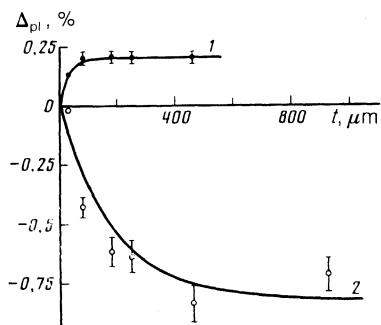


FIG. 6. The same as in Fig. 5, but for the (110) plane.

tion of the crystal thickness for electrons and positrons. The difference in the yields for the electrons increases exponentially with increasing crystal thickness, up to 100 μm . For the positrons, this difference instead decreases exponentially. Let us assume that the thickness dependence of the number of channeled particles is

$$\alpha(t) = \alpha_0 e^{-t/\lambda},$$

where α_0 is the number of particles which have been captured in a channel, and λ is the dechanneling length. The thickness dependence of the difference in the yields can then be written

$$\Delta = \Delta_0 (1 - e^{-t/\lambda}).$$

The solid lines in Figs. 5 and 6 are least-squares fits of this functional dependence to the experimental points. The dechanneling lengths for 1.2-GeV electrons in the [111] axial channel and in the (110) planar channel are 39 ± 5 and 29 ± 5 μm , respectively, in good agreement with the theoretical predictions for the [111] axis (34 μm ; Ref. 9) and for the (110) plane (about 30 μm ; Ref. 10). For positrons the dechanneling lengths for the [111] axis and the (110) plane are 210 and 190 μm , respectively, slightly lower than the 210 μm predicted theoretically⁹ for the (110) plane.

The difference between the yields for oriented and disoriented crystals arises at thicknesses at which there are channeled particles, i.e., up to 100 μm (line 1 in Fig. 5). As the crystal thickness is increased, this difference should decrease as a result of absorption. It follows from Fig. 5 that in fact this difference does not decrease anywhere up to 920 μm , so we can conclude that at large thicknesses the dechanneling of electrons is accompanied by a rechanneling process (a capture of unchanneled particles into channeling in the axial and planar cases). In the case at hand, the decrease in the yield of high-energy electrons from channeled particles due to absorption is offset by the yield of high-energy electrons from rechanneled particles. For positrons the rechanneling process is negligible at the thicknesses studied.

ORIENTATION DEPENDENCE OF THE YIELD OF HIGH-ENERGY ELECTRONS

Measurements of the high-energy component of the emission as a function of the angular orientation of the crystal with respect to the direction of the incident particles furnish an estimate of the number of channeled particles for each crystal thickness and for a given angular orientation.⁵ The transverse-energy distribution of the particles can be found from the experimental data by comparing the experi-

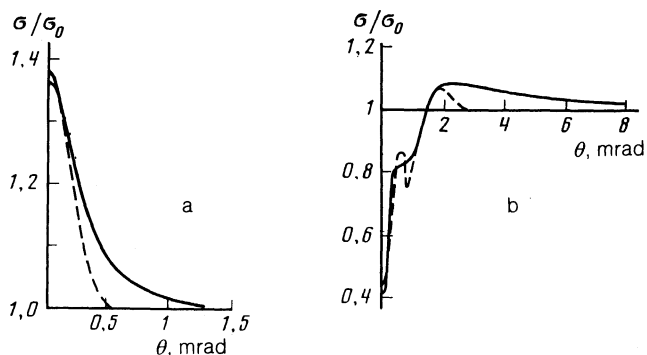


FIG. 7. Orientation dependence (normalized to the yield from an amorphous target) of the yield of high-energy electrons during the passage of (a) electrons and (b) positrons with an energy of 1.2 GeV through silicon crystals with thicknesses of (a) 80 and (b) 180 μm . Solid line—experimental; dashed line—theoretical.

mental and theoretical behavior. Figure 7 shows the orientation dependence of the yield of high-energy electrons for primary electrons and positrons, along with theoretical predictions. The solid line is experimental, and the dashed line theoretical. Below are the half-widths $\Delta_{1/2}$ of the orientation dependence for electrons and positrons; the theoretical half-widths are 0.23 mrad, the same for all the crystals:

Thickness, μm	8	30	80	180	250	460	920
$\Delta_{1/2}^-$	0.13	0.23	0.27	0.28	0.31	0.38	0.37
$\Delta_{1/2}^+$	—	0.27	0.28	0.28	0.28	0.32	0.32

It follows from these results that in the case of the electrons the width of the orientational curve depends on the thickness. Specifically, the width increases with increasing thickness. This result can be attributed to rechanneling. At a large thickness, multiple scattering may cause some of the electrons to be captured into channeling. The increase in the width of the orientation curve is significantly less pronounced in the case of positrons. This result can be attributed to the absence of a significant rechanneling at the thicknesses studied in this case.

The theoretical orientation dependences in Fig. 7 were obtained from the results of Refs. 11 and 12. The orientational dependence $\sigma(\theta)$ for the emission of high-energy electrons from the crystal, normalized to the yield σ_0 from an amorphous target can be written in the form

$$\frac{\sigma(\theta)}{\sigma_0} = \int dE g(E, \theta) \frac{1}{A(E)} \int dx dy \frac{\sigma(E, r)}{\sigma_0},$$

where $g(E, \theta)$ is the transverse-energy distribution for a given angle θ , and $A(E)$ is the accessible region in coordinate space for a given transverse energy E . For the emission of high-energy electrons the ratio $\sigma(E, r)/\sigma_0$ is equal to $\rho(r)/\rho_0$, where $\rho(r)$ is the density of electrons at a distance r from the axis of a row, and ρ_0 is the average density of electrons in the crystal. Using the Lindhard approximation,¹² we find the following expression for the electron density near the axis of a row of the crystal:

$$\rho(r) = \begin{cases} 3\rho_0 a^2 (r_0^2 + 3a^2) / (r^2 + 3a^2)^2, & E < 0 \\ \rho_0, & E > 0 \end{cases},$$

where a is a screening constant, and r_0 is the radius of the row. The transverse-energy distribution is found from

$$g(E, \theta) = \int_0^{r_0} \delta \left(E - \frac{E_0 \theta^2}{2} - U(r) \right) \frac{2r dr}{r_0^2},$$

where E_0 is the initial energy of the particle, and $U(r)$ is the screened potential of a row. In calculating the orientation dependence for the electrons we took account of dechanneling and the entry-angle distribution of the initial particles.

Channeled positrons move far from the atomic rows, in a channel formed by several rows. In this case it becomes necessary to take account of the effect of neighboring rows. The ratio of the electron densities in crystals and amorphous substances can be written

$$\frac{\rho(r)}{\rho_0} = c \sum_i [(r-r_i)^2 + 3a^2]^{-2},$$

where the sum is over all of the close-lying rows, r_i is the radius vector of row i , and

$$c = 6a^2 r_0^2 / \sum_i \left[\frac{r_0^2 - r_i^2 - 3a^2}{[r_0^4 + 2r_0^2(3a^2 - r_i^2) + (3a^2 + r_i^2)^2]^{1/2}} + 1 \right].$$

In the case of a single row, the expressions for $\rho(r)/\rho_0$ for electrons and positrons are identical.

In calculating the orientation dependence of the yield of high-energy electrons in the case of incident positrons, we take the potential of a plane to be the sum of two neighboring planes. We thus write

$$\rho(y)/\rho_0 = 3/2 a^2 (d^2 + 3a^2)^{-1/2} \{ (y^2 + 3a^2)^{-1/2} + [(d-y)^2 + 3a^2]^{-1/2} \},$$

where d is the distance between planes. The initial transverse-energy distribution for the particles emitted at an angle θ with respect to the plane is given by

$$g(E, \theta) = \int_0^d \delta \left[E - \frac{E_0 \theta^2}{2} - U(y) \right] \frac{dy}{d},$$

where $U(y)$ is the average potential of a plane.

In the calculations we ignored the dechanneling of positrons, and we took an average over the initial divergence. A comparison of the experimental and theoretical results for electrons for other crystal thicknesses showed that at small thicknesses the calculated values are larger than the experimental values at the maximum (by a factor of 1.6 for the crystals $8 \mu\text{m}$ thick), while at large thicknesses the calculated values are lower than the experimental values (by a factor

of 1.5 for the crystals $920 \mu\text{m}$ thick). A possible reason for this discrepancy is that at small thicknesses a statistical equilibrium has not yet been established, while at large thicknesses rechanneling plays a significant role.

For positrons the calculated curve gives a good description of the experimental results except at large orientation angles, $\theta > 2$ mrad. This difference may be a consequence of a dechanneling of the positrons which was ignored in the calculations for the positrons.

In summary, these results of a study of dechanneling and the orientation yields of the high-energy component of the secondary emission caused by incident electrons and positrons provide evidence that the dechanneling theory gives a good description of certain kinetic parameters characterizing the passage of a beam through a crystal. The calculated and measured dechanneling lengths agree well. It was assumed in the calculations that the decrease in the number of channeled particles is exponential. This assumption leads to a generally good quantitative description of the orientation dependence. The experimental data provide evidence of a rechanneling in the case of the electrons, especially in the thick crystals.

We wish to thank B. I. Shramenko and N. N. Nasonov for useful discussions of the experimental results.

¹V. B. Berestetskiĭ, E. M. Lifshitz, and L. P. Pitaevskii, *Kvantovaya ėlektrodinamika*, Nauka, Moscow, 1980, Part IV, pp. 357-395 (*Quantum Electrodynamics*, Pergamon, Oxford, 1982).

²B. Planskov, *Nucl. Instrum. Meth.* **24**, 172 (1963).

³V. A. Gol'dshtein, I. M. Arkatov, and V. I. Startsev, *Prib. Tekh. Eksp.* No. 2, 50 (1971).

⁴G. D. Kovalenko, *Ukr. Fiz. Zh.* **26**, 1839 (1981).

⁵D. I. Adejshvili, G. L. Bochek, V. I. Vit'ko, *et al.*, *Radiat. Eff. Lett.* **87**, 135 (1985).

⁶I. A. Grishaev, G. D. Kovalenko, and B. I. Shramenko, *Pis'ma Zh. Tekh. Fiz.* **5**, 1104 (1979) [*Sov. Tech. Phys. Lett.* **5**, 461 (1979)].

⁷E. Raquet, Preprint DESY-69/12, 1969, p. 9.

⁸V. J. Vanhuyse and R. E. Vandevijer, *Nucl. Instrum. Methods* **15**, 63 (1962).

⁹V. A. Muralev, *Nucl. Instrum. Methods* **230**, 51 (1984).

¹⁰R. Wedell, *Phys. Status Solidi* **b99**, 11 (1980).

¹¹J. Lindhard, *Mat.-Fyz. Medd. Dan. Vid. Selsk.* **34**, No. 14 (1965) [*Russ. transl. Usp. Fiz. Nauk* **99**, 249 (1969)].

¹²J. F. Bak, G. Melchart, S. P. Moller, *et al.*, *Nucl. Phys.* **A389**, 533 (1982).

Translated by Dave Parsons